



**CHALMERS**  
UNIVERSITY OF TECHNOLOGY

## **Comparative Study of SO<sub>2</sub> and SO<sub>2</sub>/SO<sub>3</sub> Poisoning and Regeneration of Cu/BEA and Cu/SSZ-13 for NH<sub>3</sub> SCR**

Downloaded from: <https://research.chalmers.se>, 2022-10-11 19:36 UTC

Citation for the original published paper (version of record):

Auvray, X., Arvanitidou, M., Högström, Å. et al (2021). Comparative Study of SO<sub>2</sub> and SO<sub>2</sub>/SO<sub>3</sub> Poisoning and Regeneration of Cu/BEA and Cu/SSZ-13 for NH<sub>3</sub> SCR. *Emission Control Science and Technology*, 7(4): 232-246. <http://dx.doi.org/10.1007/s40825-021-00203-4>

N.B. When citing this work, cite the original published paper.



# Comparative Study of SO<sub>2</sub> and SO<sub>2</sub>/SO<sub>3</sub> Poisoning and Regeneration of Cu/BEA and Cu/SSZ-13 for NH<sub>3</sub> SCR

Xavier Auvray<sup>1</sup> · Maria Arvanitidou<sup>1</sup> · Åsa Högstöm<sup>1</sup> · Jonas Jansson<sup>2</sup> · Sheedeh Fouladvand<sup>2</sup> · Louise Olsson<sup>1</sup>

Received: 3 May 2021 / Revised: 15 September 2021 / Accepted: 10 October 2021  
© The Author(s) 2021

## Abstract

Two copper-exchanged zeolites, Cu/SSZ-13 and Cu/BEA, were studied as catalysts for the selective reduction of NO<sub>x</sub> by NH<sub>3</sub> (NH<sub>3</sub>-SCR). Their activities for standard SCR (NO<sub>x</sub>=NO) and fast SCR (NO<sub>x</sub>=50% NO+50% NO<sub>2</sub>) were measured before and after sulfur poisoning at 250 °C. The effect of 30 ppm SO<sub>2</sub> and a mixture of 24 ppm SO<sub>3</sub>+6 ppm SO<sub>2</sub> was evaluated. The repetition of subsequent activity measurements served as regeneration method in SCR conditions. SO<sub>2</sub> deactivated Cu/SSZ-13 whereas Cu/BEA was only moderately affected. SO<sub>3</sub> led to stronger deactivation of both catalysts than SO<sub>2</sub>. However, also for this case, the Cu/BEA was significantly less affected than Cu/SSZ-13, even though Cu/BEA contained larger amount of stored sulfur. One possible reason for this could be the large pores of Cu/BEA, where the sulfur species possibly resulted in less sterical hindrance than in the small pore SSZ-13 structure. NH<sub>3</sub> temperature-programmed desorption (NH<sub>3</sub>-TPD) showed no loss of storage sites upon sulfur treatment and subsequent regeneration. Partial activity recovery was observed after a period in SCR conditions at 400 °C and 500 °C. Temperature at 300 °C was insufficient to regenerate the catalysts. Diffuse reflectance infrared Fourier transform spectroscopy (DRIFTS) of NO adsorption suggested that SO<sub>2</sub> interacts with the ZCuOH sites on Cu/SSZ-13, causing the strong poisoning.

**Keywords** NH<sub>3</sub> SCR · Poisoning · SO<sub>2</sub> and SO<sub>3</sub> · Cu/zeolites

## 1 Introduction

Diesel and lean-burn gasoline engines present the advantage to be more fuel-efficient and to emit less CO<sub>2</sub> than gasoline engines. However, these combustion systems also produce nitrogen oxides (NO<sub>x</sub>). NH<sub>3</sub>-SCR is an efficient process to reduce NO<sub>x</sub> by NH<sub>3</sub> over a metal-exchanged zeolite or V<sub>2</sub>O<sub>5</sub>-based catalyst. For automotive applications, NH<sub>3</sub> can be produced in situ through decomposition and hydrolysis of a solution of urea sprayed in the exhaust gas.

The exhaust gas contains other chemical compounds that can interfere with the NH<sub>3</sub>-SCR process and deactivate the widely used, efficient, Cu-exchanged zeolite catalyst. Sulfur oxides (SO<sub>x</sub>) are impactful poisons which are therefore

widely studied. Even at low concentration, the SO<sub>x</sub> store and accumulate on the catalyst. They can block the active sites for the NO<sub>x</sub> reduction reaction and decrease the catalytic performance with time [1–5]. This accumulation process requires periodic regeneration of the catalyst. Reducing conditions and high-temperature treatment can readily decompose the stored SO<sub>x</sub> species. However, such reducing conditions at a high temperature may permanently damage the Cu-exchanged zeolite catalyst [6]. To preserve the catalyst, it is important to further develop regeneration strategies for SO<sub>x</sub>-poisoned SCR catalysts.

Most of the SO<sub>x</sub> poisoning and regeneration studies solely focus on the impact of SO<sub>2</sub> as SO<sub>x</sub> species and thermal regeneration [3, 5, 7–12], sometimes carried out under reducing atmosphere. However, the SO<sub>2</sub> present in the exhaust of a modern vehicle passes through an oxidation catalyst before reaching the SCR catalyst. The oxidation catalyst is a noble metal-based catalyst which oxidizes CO and hydrocarbons into CO<sub>2</sub> and water vapor. It also oxidizes a large fraction of NO to NO<sub>2</sub> and SO<sub>2</sub> to SO<sub>3</sub> [13–16]. The oxidation of SO<sub>3</sub> occurs also on the Cu/SSZ-13 SCR catalyst itself from 450 °C [9]. Therefore, it is relevant to study the

✉ Louise Olsson  
louise.olsson@chalmers.se

<sup>1</sup> Chemical Engineering, Competence Centre for Catalysis, Chalmers University of Technology, S-412 96 Gothenburg, Sweden

<sup>2</sup> Volvo Group Trucks Technology, SE-405-08, Gothenburg, Sweden

impact of a  $\text{SO}_2/\text{SO}_3$  mixture on SCR catalysts because it is more representative of the real conditions.  $\text{SO}_3$  reacts readily with  $\text{NH}_3$  to form a solid salt that decomposes at a high temperature. Moreover,  $\text{SO}_3$  has shown a higher potential to store and deactivate the SCR catalyst than  $\text{SO}_2$  [17–19]. Simultaneous sulfur poisoning and thermal aging was studied by Wijayanti et al. [12] using  $\text{SO}_2$  and Tang et al. [20] using a  $\text{SO}_x$  mixture containing a large amount of  $\text{SO}_3$ . Tang et al. [20] found that a hydrothermal pretreatment prior to sulfur exposure can decrease the deactivation of the SCR catalyst.

The zeolite structure also affects the sulfur aging for Cu/zeolites as found in one of our earlier studies, where Cu/SSZ-13 and Cu/LTA were compared during sulfur poisoning with  $\text{SO}_2$  [11]. However, there are according to the best of our knowledge no studies available where the effect of zeolite structure in Cu/zeolites is examined for sulfur poisoning using both  $\text{SO}_2$  and  $\text{SO}_3$  as a  $\text{SO}_x$  source. In this work, we therefore performed the comparative poisoning of two kinds of Cu-exchanged zeolites with  $\text{SO}_2$  and a mixture of  $\text{SO}_2/\text{SO}_3$ . The influence of the zeolite structure (SSZ-13 and BEA) was thus studied and the impact of  $\text{SO}_3$  was determined and compared with the impact of  $\text{SO}_2$ . The regeneration of poisoned catalyst was performed at various temperatures under realistic SCR conditions. Both the standard SCR and fast SCR activities were evaluated. The fresh and poisoned catalysts were characterized by XRD, ICP, and BET surface measurement.

## 2 Experimental Methods

### 2.1 Catalyst Synthesis

Two zeolite types were studied, where the BEA zeolite was commercial (Zeolyst International, Si/Al=19) while the SSZ-13 (chabazite structure) was synthesized. The SSZ-13 was chosen since Cu/SSZ-13 has been used for removing  $\text{NO}_x$  from diesel vehicles for several years [21]. In order to aid the understanding of the poisoning and regeneration ability of Cu/SSZ-13, we compare it with another Cu/zeolite, namely Cu/BEA due to the high activity of Cu/BEA for SCR with  $\text{NH}_3$ . It should be noted that Cu/BEA is not commercially applicable due to thermal degradation [22] and hydrocarbon poisoning [23] issues and was chosen in this work for mechanistic reasons together with Cu/SSZ-13.

The chabazite structure was obtained by hydrothermal conversion of a faujasite zeolite. NaOH pellets (Sigma-Aldrich > 98% anhydrous pellets) were dissolved in deionized water (Millipore) to prepare a 1 M NaOH solution. Sodium trisilicate ( $\text{Na}_2\text{SiO}_3$ , VWR) and deionized water were added to the NaOH solution under stirring. The respective proportions used were 250 g and 320 g for a 200 mL

NaOH solution. After 15 min stirring, 25 g of faujasite zeolite were added (Zeolyst International, CBV720). The solution was stirred for 30 min at room temperature before addition of 105 g of the structure-directing agent (SDA), N,N,N-trimethyl-1-adamantanamine iodide (TMAAI, Zeo-Gen SDA 2825). After 30 min under stirring at room temperature, the mixture was transferred to the Teflon liner of a stainless-steel autoclave (Parr Instrument Company) for hydrothermal treatment. The autoclave was then placed in a static oven at 140 °C for 6 days. The mixture was centrifuged to collect the solid zeolite. The zeolite was then washed with deionized water and again collected by centrifugation. The pH of the liquid after washing was measured and the washing process was repeated until this pH was neutral. The zeolite was dried at room temperature for at least 12 h and calcined for 8 h at 550 °C with a slow heating rate of 0.5 °C/min. The sodium form of the zeolite (Na/SSZ-13), where  $\text{Na}^+$  cations counterbalance the negative charge of the aluminum, was thus obtained.

The next step in the catalyst preparation was ion exchange. Similar ion exchange procedure was applied to both BEA and CHA zeolites. Sodium ions were exchanged by ammonium ions with a solution of ammonium nitrate (2 M) prepared by dissolving  $\text{NH}_4\text{NO}_3$  (Sigma-Aldrich, > 99.0%) in deionized water. The zeolite powder was poured into the ammonium nitrate solution (33.33 mL/g of zeolite) and heated in an oil bath at 80 °C for 15 h under stirring. The powder was collected and washed as described previously. After drying at room temperature for at least 12 h, a second exchange with  $\text{NH}_4\text{NO}_3$  was performed in the same way. After washing and drying (12 h at room temperature), the zeolite was added to a copper nitrate solution (0.2 M, 33.33 mL/g of zeolite) for the copper exchange stage. The copper nitrate solution was prepared by dissolving copper nitrate hemi(penta-hydrate) ( $\text{CuN}_2\text{O}_6 \cdot 2.5\text{H}_2\text{O}$ , Sigma-Aldrich) in deionized water. The mixture was maintained under vigorous stirring at 80 °C in an oil bath for 2 h. After washing and drying, the Cu-exchanged zeolite was calcined for 4 h at 550 °C with a heating rate of 5 °C/min.

For activity studies and poisoning in synthetic gas bench reactor (SGB), catalyst-coated monoliths were prepared. The cordierite honeycomb substrate (Corning) had a channel density of 400 cpsi and was calcined at 600 °C for 2 h prior to coating. The monoliths were 20 mm long with a diameter of 15 mm for a volume of ca. 3.5 mL. The washcoat was made of 5 wt% boehmite (Disperal P2, Sasol) and 95 wt% catalyst. The washcoat powder was dispersed in a solution of 50 wt% deionized water and 50 wt% spectroscopic purity grade ethanol (Merck) with a liquid-to-solid mass ratio of 4. The cordierite substrate was dipped into the slurry to fill up the channels. The solvent was evaporated under a hot air gun while rotating manually the sample to ensure homogeneous coating. The process was repeated until 300 mg washcoat

was loaded on the substrate. Finally, the samples were calcined in air at 500 °C for 2 h.

## 2.2 Characterization Methods

The crystalline structure of the zeolites was examined by X-ray diffraction with a powder diffractometer (Siemens D5000) operating at 40 kV, using the  $K\alpha_1$  emission ray of a Cu anode as the X-ray source ( $\lambda = 1.54060 \text{ \AA}$ ). The X-ray diffraction angle was measured in the Bragg–Brentano geometry. The elemental composition of the catalyst was determined by ICP-AES (ALS Scandinavia). The specific surface area was measured by physisorption of  $N_2$  at 77 K with a Micromeritics Tri-Star 3000 and calculated according to the BET method.

## 2.3 DRIFT Spectroscopy of NO Adsorption

NO adsorption was conducted on degreened and  $SO_2$ -poisoned monolithic catalysts treated in the flow reactor described below. The monoliths were crushed into a powder and then sieved to keep the particles fraction between 40 and 80  $\mu\text{m}$ . The catalyst was placed in the sample holder of a heated Praying Mantis DRIFT cell (Harrick Scientific Products, Pleasantville, NY, USA) equipped with ZnSe windows and mounted on a Vertex 70 FTIR spectrometer (Bruker, Billerica, MA, USA) equipped with a liquid  $N_2$ -cooled MCT detector. The spectra were recorded with a resolution of  $4 \text{ cm}^{-1}$ . Before NO adsorption, the sample was firstly pretreated with 8%  $O_2$  at 500 °C for 45 min and cooled to 30 °C. Ar was then flushed over the sample for 60 min at 30 °C and a background spectrum was recorded under these conditions (32 scans). The total gas flow rate was always 50 mL/min with Ar as balance gas. A total of 500 ppm NO in Ar was then fed to the catalyst bed at 30 °C for 60 min. Spectra (12 scans) were recorded with a 5-min interval during NO adsorption.

## 2.4 Reactor Setup

These experiments were performed in a reactor made of a horizontal quartz tube heated by a resistance coil. The assembly was wrapped in quartz wool for insulation. The monolith was placed at ca. 9 cm from the tube outlet and wrapped in a layer of quartz wool to fill the void between the monolith and the reactor wall and thus avoid gas bypassing. Two thermocouples were inserted from the reactor outlet to record the intra-catalyst temperature and the inlet gas temperature (ca. 0.5 cm in front of the monolith). The thermocouple measuring the inlet gas temperature was used as feedback to regulate the reactor temperature. The gases were delivered by mass flow controllers (Bronkhorst) and the water vapor flow was generated by a controlled evaporator

mixer (Bronkhorst). The outlet gas composition was quantitatively determined by a gas FTIR spectrometer equipped with a liquid  $N_2$ -cooled MCT detector, a gas cell with a 5.11 m effective pathlength, and ZnSe windows (MultiGas 2030, MKS Instruments). The operating temperature of the spectrometer and of the inlet and outlet gas lines was 191 °C.

## 2.5 Activity Measurements

The samples were first subjected to a degreening step at 600 °C for 3 h. The gas flow composition for the degreening was 400 ppm NO, 400 ppm  $NH_3$ , 8%  $O_2$ , and 5%  $H_2O$  balanced in Ar. After this, activity measurement was done in standard SCR conditions (400 ppm NO, 400 ppm  $NH_3$ , 8%  $O_2$ , 5%  $H_2O$  balanced in Ar) and fast SCR conditions (200 ppm NO, 200 ppm  $NO_2$ , 400 ppm  $NH_3$ , 8%  $O_2$ , 5%  $H_2O$  balanced in Ar). Prior to the standard and fast SCR activity measurements, the catalyst was pre-treated at 500 °C for 20 min in a gas flow of 8%  $O_2$  and 5%  $H_2O$  balanced in Ar. This pre-treatment was not applied after poisoning to observe solely the effect of the regeneration in SCR conditions. The standard SCR activity was measured stepwise with a 30-min-long step at each temperature. When necessary, the steps were extended to 45 min to ensure steady-state measurement. For the degreened catalysts, the activity was measured at 100, 125, 150, 175, 200, 250, 300, 350, 400, 450, and 500 °C. The fast SCR activity was measured at 175, 200, 250, 300, 350, 400, 450, and 500 °C with 45-min-long steps. In all experiments, argon was used as carrier gas and the total flow rate was 1.2 L/min ( $GHSV = 20,400 \text{ h}^{-1}$ ).

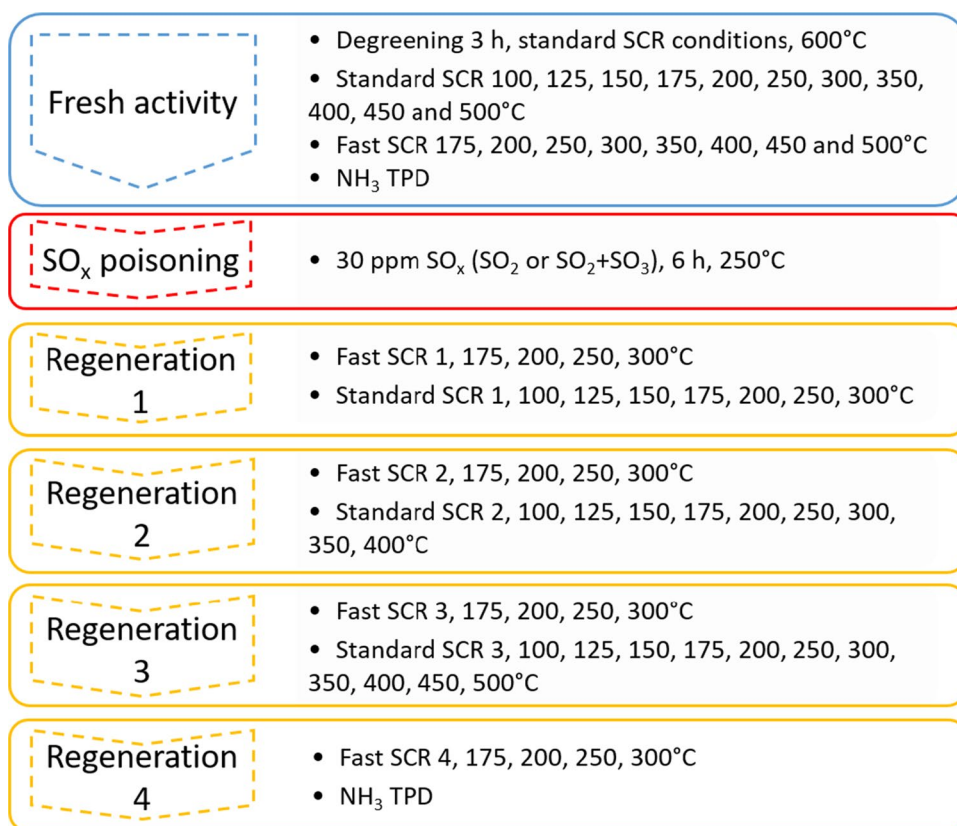
## 2.6 $NH_3$ TPD

After degreening and activity measurement, temperature-programmed desorption of  $NH_3$  was conducted in the same reactor to measure the amount and strength of the different  $NH_3$  storage sites. The catalyst was exposed to 400 ppm  $NH_3$  and 5%  $H_2O$  in Ar for 90 min at 200 °C. The catalyst was then flushed with 5%  $H_2O$  in Ar for 1 h at 200 °C before ramping the temperature at 10 °C/min up to 600 °C.  $NH_3$  TPD was also carried out after  $SO_x$  poisoning and regeneration (Fig. 1).

## 2.7 Poisoning

$SO_2$  and  $SO_2/SO_3$  poisoning was carried out for 6 h at 250 °C with a gas flow containing 30 ppm  $SO_x$ , 400 ppm NO, 8%  $O_2$ , and 5%  $H_2O$  balanced in Ar.  $NH_3$  was preadsorbed on the catalyst for 30 min at 250 °C (800 ppm  $NH_3$ , 5%  $H_2O$  balanced in Ar).  $SO_3$  was produced by oxidation of  $SO_2$  over a 7.7 wt% Pt/ $Al_2O_3$  catalyst that was placed in a separate tubular reactor fed with  $SO_2$ ,  $O_2$  flows, and Ar. During  $SO_2/SO_3$  poisoning, all gases passed through

**Fig. 1** Schematic diagram of the experimental procedure conducted on monolithic catalysts in SGB reactor.  $\text{SO}_x$  poisoning: 30 ppm  $\text{SO}_x$ , 400 ppm NO, 8%  $\text{O}_2$ , 5%  $\text{H}_2\text{O}$  balanced in Ar. Standard SCR: 400 ppm NO, 400 ppm  $\text{NH}_3$ , 8%  $\text{O}_2$ , 5%  $\text{H}_2\text{O}$  balanced in Ar. Fast SCR: 200 ppm NO, 200 ppm  $\text{NO}_2$ , 400 ppm  $\text{NH}_3$ , 8%  $\text{O}_2$ , 5%  $\text{H}_2\text{O}$  balanced in Ar



the  $\text{SO}_3$  generator except NO, water vapor, and argon used to carry water vapor. The  $\text{SO}_3$  generator temperature was set to 550 °C corresponding to a thermodynamic equilibrium of 80%  $\text{SO}_3$ . Assessment of the  $\text{SO}_2$  oxidation was made in an empty reactor. The concentrations measured at the outlet were 24 ppm  $\text{SO}_3$  and 6 ppm  $\text{SO}_2$  for a feed containing 30 ppm  $\text{SO}_2$  and 8%  $\text{O}_2$  in Ar. The system was therefore able to generate  $\text{SO}_3$  according to the thermodynamic levels. The  $\text{SO}_3$  generator outlet was connected to the inlet line of the main reactor as close as possible to the reactor inlet and all lines were carefully heated with electrical heating bands. Ultra-low sulfur diesel (ULSD) contains a maximum mass fraction of 15 ppm sulfur (in the USA). The combustion of such fuel emits  $\text{SO}_2$  in a concentration that inherently depends on the air-to-fuel ratio (A/F) and can be calculated. For diesel vehicles, A/F varies a lot depending on driving conditions and engine load. Assuming A/F = 25, the combustion of ULSD yields  $\text{SO}_2 = 0.518\text{ppmv}$ . In these conditions, our poisoning corresponds to the sulfur emission of a ca. 300 h driving cycle. It should be noted that the assumed A/F is rather low so the engine out  $\text{SO}_2$  concentration can be even lower.

## 2.8 Regeneration

The regeneration procedure consisted in repeating the standard and fast SCR activity measurements described previously. However, at each repetition of standard SCR, measurement steps were added at a higher temperature. Thus, the effect of the added temperature step, in SCR conditions, could affect the subsequent fast SCR and standard SCR activity measurements. A complete diagram of the experiments is shown in Fig. 1.

## 3 Results and Discussion

### 3.1 Catalyst Characterization

Table 1 shows the Cu loading and the Si and Al content of the catalysts according to ICP-AES measurements. Cu/SSZ-13 exhibited a Cu loading of 1.7 wt% and a Si/Al molar ratio of 17 which corresponds to a Cu/Al ratio of 0.30. The Cu loading of Cu/BEA was 1.9 wt% and its Si/Al ratio was 19, corresponding to a Cu/Al ratio of 0.39. The sulfur loading



**Table 1** Elemental composition of Cu/SSZ-13 and Cu/BEA determined by ICP-AES

| Fresh powder  | Cu/BEA | Cu/SSZ-13 |
|---|--------|-----------|
| Copper loading (wt%)  | 1.9    | 1.7       |
| Si/Al ratio   | 19     | 17        |
| S content after SO <sub>2</sub> poisoning (wt%)               |        |           |
| Crushed monolith (measured, based on crushed monolith)        | 0.11   | 0.01      |
| Catalyst washcoat (calculated, based on only washcoat weight) | 0.45   | 0.04      |

**Table 2** BET surface area of fresh and SO<sub>2</sub>-poisoned Cu/SSZ-13 and Cu/BEA

| BET surface area (m <sup>2</sup> /g) | Cu/BEA | Cu/SSZ-13 |
|--------------------------------------|--------|-----------|
| Fresh calcined powder                | 621    | 692       |
| Degreened monolith*                  | 128    | 167       |
| Poisoned monolith*                   | 124    | 163       |

\*Crushed monolith, including both washcoat and cordierite

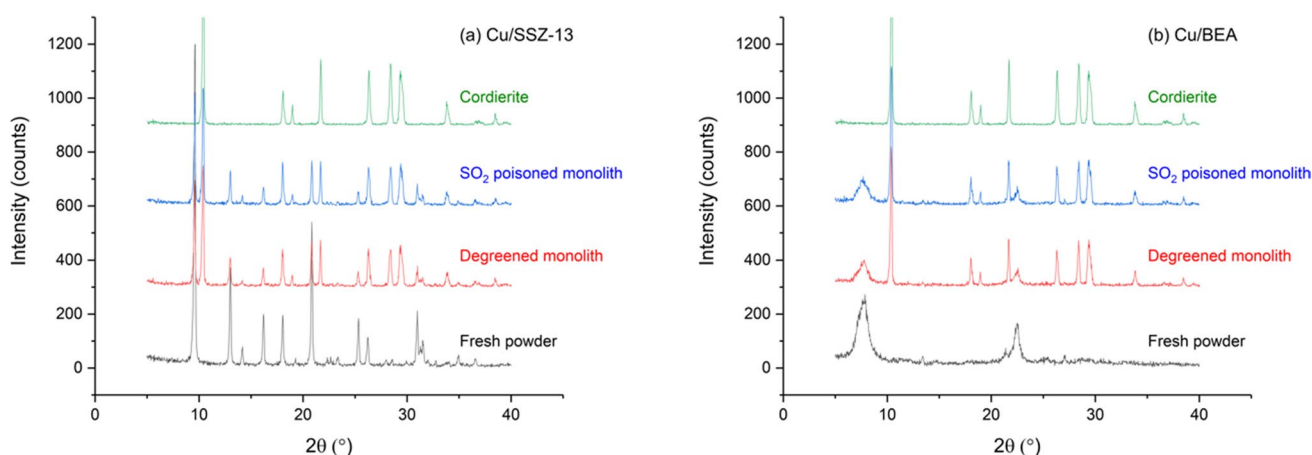
after SO<sub>2</sub> poisoning was also measured on crushed monolithic samples specially prepared for characterization. They were degreened and treated with SO<sub>2</sub> in the same reactor and according to the same procedure as the other samples used for activity measurements. It is clear that the Cu/BEA contained significantly more sulfur after poisoning compared to Cu/SSZ-13 (see Table 1).

Table 2 reports the BET surface area of the calcined fresh powders and the degreened and SO<sub>2</sub>-poisoned monoliths which were crushed for the analysis. For the calcined powders, the Cu/SSZ-13 exhibited a slightly higher BET surface area. Crushed monoliths had significantly lower surface area than its corresponding catalyst powder. This is due to the

dilution of the catalyst with crushed cordierite, since the specific surface area of cordierite substrate was negligible (0.7 m<sup>2</sup>/g). Moreover, the surface area before and after SO<sub>2</sub> poisoning was similar for both catalysts, suggesting no significant blocking of the pores by sulfur deposits (Table 2). The sulfur content measured after SO<sub>2</sub> poisoning confirmed the sulfur deposition on both catalysts.

Figure 2 shows the X-ray diffractograms obtained with the Cu/SSZ-13 (a) and the Cu/BEA (b) catalysts. The diffractograms of the fresh powders are shown to evaluate the structure and the crystallinity. The diffractograms of the respective degreened and poisoned crushed monolith are shown with an offset. The diffractogram of the cordierite substrate is also given as a reference. Figure 2a shows sharp peaks at  $2\theta = 9^\circ, 13^\circ, 16^\circ, 18^\circ, 21^\circ, 25^\circ,$  and  $31^\circ$  corresponding to the chabazite structure [5, 6, 24]. Those characteristic peaks were detected with the degreened and SO<sub>2</sub>-poisoned monoliths which shows that the zeolite structure was not altered by the coating process, the degreening, and the poisoning. The results also clearly show that all FAU was converted to CHA during synthesis, since the peak at  $6.3^\circ$  [25] is absent. Crystalline copper was not detected by XRD which rules out the presence of large copper particles. It rather suggests that copper is well-dispersed, as desired. Figure 2b shows analogous results in the case of Cu/BEA. The fresh powder shows a broad feature at  $2\theta = 7.6^\circ, 22.5^\circ$  corresponding to the BEA zeolite structure. No other diffraction peaks were detected, indicating that the copper was well-dispersed. The BEA zeolite is partially disordered which is confirmed by the large width of the peaks measured. Like for SSZ-13, the degreening and the SO<sub>2</sub> poisoning did not damage the structure of the BEA zeolite, which is in line with the surface area measurements (Table 2).

Figure 3 reports the NH<sub>3</sub> release during NH<sub>3</sub>-TPD for the degreened, SO<sub>2</sub>-poisoned, and SO<sub>3</sub>-poisoned catalysts.

**Fig. 2** XRD patterns of the fresh powders, the degreened crushed monoliths, and the SO<sub>2</sub>-poisoned crushed monoliths. **a** Cu/SSZ-13 and **b** Cu/BEA

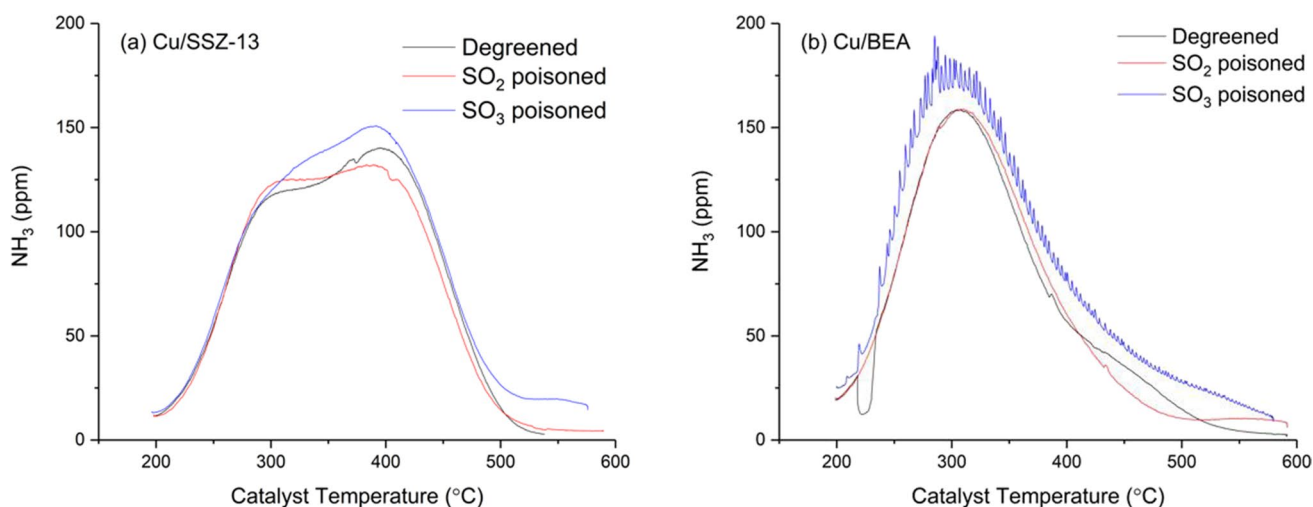


**Fig. 3**  $\text{NH}_3$ -TPD profiles of degreened,  $\text{SO}_2$ -poisoned (and regenerated), and  $\text{SO}_3$ -poisoned (and regenerated) **a** Cu/SSZ-13 and **b** Cu/BEA. Feed: 5%  $\text{H}_2\text{O}$  in Ar, flowrate=1.2L/min, ramping rate: 10 °C/

min. During  $\text{SO}_2$  poisoning, 30 ppm  $\text{SO}_2$  was used, and during  $\text{SO}_3$  poisoning, 24 ppm  $\text{SO}_3$  and 6 ppm  $\text{SO}_2$ , in the presence of 400 ppm NO, 8%  $\text{O}_2$ , 5%  $\text{H}_2\text{O}$  for both cases

Figure 3a presents the typical binodal  $\text{NH}_3$  profile of Cu/SSZ-13, constituted of two main peaks. The low-temperature release, centered at 300 °C, was assigned to  $\text{NH}_3$  adsorbed on exchanged copper ions which are Lewis acid sites [6, 26]. The high-temperature peak was assigned to  $\text{NH}_3$  adsorbed on the stronger sites, i.e., the Brønsted acid sites of the zeolite and, in lesser extent, the strongest of the Lewis sites [6, 27]. The  $\text{NH}_3$  TPD after  $\text{SO}_2$  and  $\text{SO}_3$  poisoning was performed after all regeneration steps (see Fig. 1); thus, a large amount of sulfur was likely already removed. After  $\text{SO}_2$  poisoning and regeneration, the amount of  $\text{NH}_3$  stored was similar. However,  $\text{SO}_2$  poisoning slightly changed the binding strength, indicated by the larger low-temperature

peak and the smaller high-temperature peak. Wijayanti et al. [5] found that sulfur adsorption could induce new ammonia storage sites in Cu/SSZ-13, and this might be the reason for the small shift in binding strength of the ammonia in our results (see Fig. 3a). Interestingly,  $\text{SO}_3$  poisoning and regeneration increased the  $\text{NH}_3$  storage, which is in line with the results by Wijayanti et al. [5] and Brookshear et al. [8] using  $\text{SO}_2$ . In addition, a desorption feature at 555 °C was observed and was correlated to a sulfur release (Fig. 4a). The additional stored ammonia can have formed ammonium sulfate or ammonium bisulfate with the adsorbed sulfur [8, 28]. As shown in Fig. 4a,  $\text{SO}_2$  was released during the  $\text{NH}_3$ -TPD. Both Cu/SSZ-13 samples showed one peak at 400 °C and

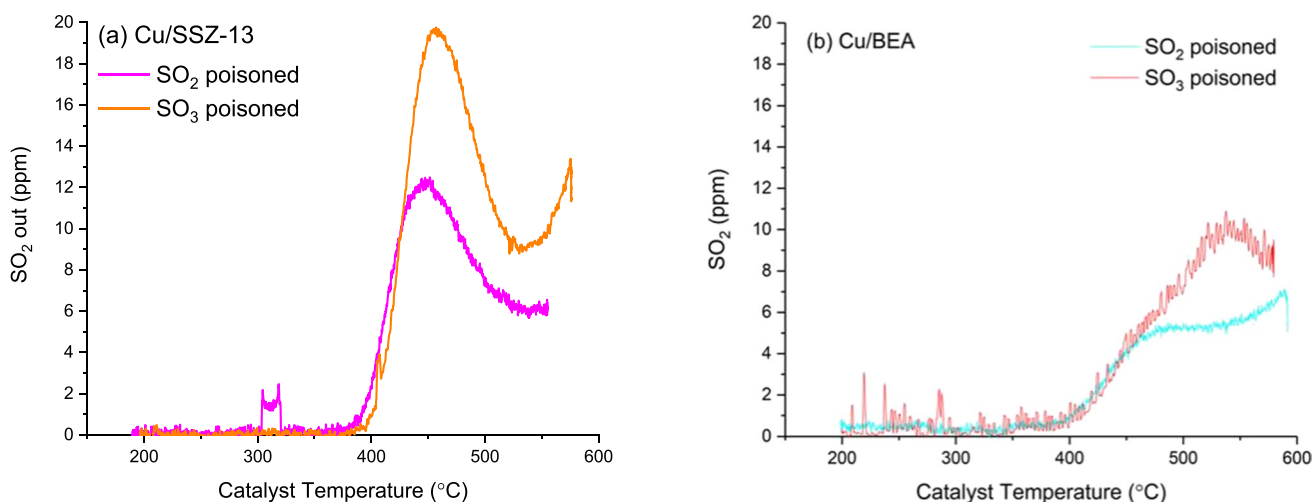


**Fig. 4**  $\text{SO}_2$  desorption during  $\text{NH}_3$ -TPD carried out on  $\text{SO}_2$ -poisoned (and regenerated) and  $\text{SO}_3$ -poisoned (and regenerated) **a** Cu/SSZ-13 and **b** Cu/BEA. Feed: 5%  $\text{H}_2\text{O}$  in Ar, flowrate=1.2L/min, ramping

rate: 10 °C/min. During  $\text{SO}_2$  poisoning, 30 ppm  $\text{SO}_2$  was used, and during  $\text{SO}_3$  poisoning, 24 ppm  $\text{SO}_3$  and 6 ppm  $\text{SO}_2$ , in the presence of 400 ppm NO, 8%  $\text{O}_2$ , 5%  $\text{H}_2\text{O}$  for both cases

the  $\text{SO}_3$ -poisoned catalyst showed an additional incomplete peak starting to form at 550 °C. This is consistent with the  $\text{SO}_2$  desorption observed by Wijayanti et al. [12] at 540 and 780 °C, after  $\text{SO}_2$  poisoning of Cu/SSZ-13. The  $\text{SO}_2$  release measured was greater for the  $\text{SO}_3$ -poisoned catalyst, indicating larger sulfur storage for the  $\text{SO}_3$  poisoned case. However, it should be noted that it is possible that the sulfates also are released as  $\text{SO}_3$  or  $\text{H}_2\text{SO}_4$ , but these species were not measured. The study of the stored sulfur species by Su et al. [4] revealed three distinct types of sulfur species, the thermal decomposition of which releases  $\text{SO}_2$ . They observed desorption features peaking at 545, 632, and 772 °C, assigned to  $\text{H}_2\text{SO}_4$ ,  $\text{CuSO}_4$ , and  $\text{Al}_2(\text{SO}_4)_3$ , respectively. Since we observe a sulfur desorption starting from 550 °C, it could possibly be related to the decomposition of  $\text{H}_2\text{SO}_4$  adsorbed on the catalyst, in line with the work by Su et al. [4].

The  $\text{NH}_3$ -TPD of Cu/BEA showed one main peak at 310 °C and the degreened catalyst showed a shoulder at 450 °C which was absent after  $\text{SO}_2$  poisoning. A weak peak at 560 °C can be observed on the  $\text{SO}_2$ -poisoned catalyst and a shoulder at 530 °C was present after  $\text{SO}_3$  poisoning. In general, the  $\text{NH}_3$  storage was not decreased with sulfur poisoning and regeneration. Like for Cu/SSZ-13, the  $\text{NH}_3$  release was even enhanced with  $\text{SO}_3$  exposure and small amounts of  $\text{SO}_2$  were released from 400 °C (Fig. 4b). A first  $\text{SO}_2$  peak appeared at 475 °C on the  $\text{SO}_2$ -poisoned Cu/BEA. This peak appeared as a shoulder on the  $\text{SO}_3$ -poisoned Cu/BEA and was probably due to ammonium sulfate decomposition. A second peak was observed at 540 °C on the  $\text{SO}_3$ -poisoned Cu/BEA and at a temperature higher than 600 °C on the  $\text{SO}_2$ -poisoned Cu/BEA. These peaks demonstrated the formation of different sulfate species such as  $\text{H}_2\text{SO}_4$ ,  $\text{CuSO}_4$  depending on the sulfur feed used during

poisoning. This result is consistent with the influence of SCR conditions and  $\text{H}_2\text{O}$  on the amount and partition of sulfate species demonstrated by Su et al. [4].

To summarize, the catalyst characterization indicates that the physical properties of the catalysts were almost unaffected by the  $\text{SO}_x$  treatments. The  $\text{SO}_2$  desorption observed during  $\text{NH}_3$ -TPD at the end of the poisoning and regeneration procedure indicates that some stored sulfur species remained despite the regeneration.

### 3.2 Standard SCR Activity for Degreened and Poisoned Samples

Figure 5 is a comparative graph reporting the steady-state conversion of NO measured at several temperatures in the range of 100–500 °C. The curves depict the standard SCR activity for the degreened catalysts, after  $\text{SO}_2$  poisoning and after  $\text{SO}_3/\text{SO}_2$  poisoning (denoted  $\text{SO}_3$  poisoning). The activity of Cu/SSZ-13 is reported in Fig. 5a, which also includes the results for the degreened Cu/BEA. Both degreened catalysts show similar activity characterized by a low NO conversion below 150 °C, a conversion greater than 90% between 250 and 350 °C, and the slight decline of the conversion at  $T > 350$  °C. After  $\text{SO}_2$  poisoning, the light-off temperature increased, but even more so after  $\text{SO}_3$  poisoning. For example, the NO conversion was 51% at 250 °C and 81% at 300 °C for  $\text{SO}_2$  poisoned Cu/SSZ-13, while after  $\text{SO}_3/\text{SO}_2$  poisoning, the NO conversion at 300 °C was only 44%. The results in Fig. 5a clearly demonstrate the high sensitivity of Cu/SSZ-13 to  $\text{SO}_2$  and, to a greater extent, to  $\text{SO}_3$ . It should be noted that  $\text{N}_2\text{O}$  was also formed during SCR, even more so during fast SCR, and that  $\text{SO}_2$  and  $\text{SO}_3$  significantly decreased the  $\text{N}_2\text{O}$  formation (data not shown).

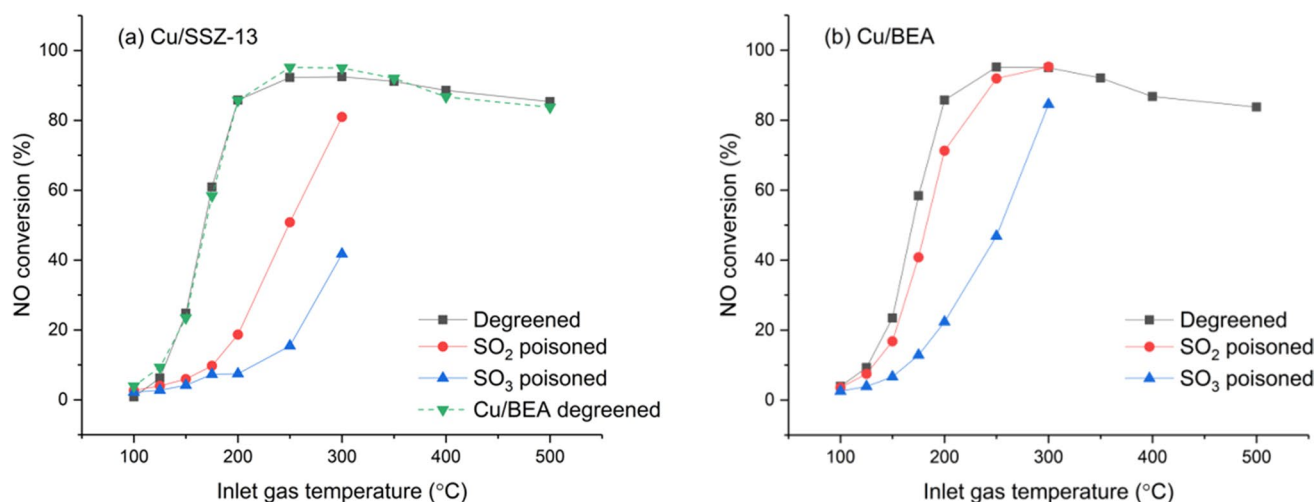


**Fig. 5** Standard SCR activity (NO conversion) of degreened,  $\text{SO}_2$ -poisoned, and  $\text{SO}_3$ -poisoned **a** Cu/SSZ-13 and **b** Cu/BEA. Feed: 400 ppm NO, 400 ppm  $\text{NH}_3$ , 8%  $\text{O}_2$ , 5%  $\text{H}_2\text{O}$  in Ar, flowrate=1.2L/min.

During  $\text{SO}_2$  poisoning, 30 ppm  $\text{SO}_2$  was used, and during  $\text{SO}_3$  poisoning, 24 ppm  $\text{SO}_3$  and 6 ppm  $\text{SO}_2$ , in the presence of 400 ppm NO, 8%  $\text{O}_2$ , 5%  $\text{H}_2\text{O}$  for both cases



The impact of  $\text{SO}_2$  and  $\text{SO}_3$  poisoning on the SCR activity of Cu/BEA is compared in Fig. 5b. Also, for this catalyst, the NO conversion dropped at 175 and 200 °C after  $\text{SO}_2$  poisoning. However, the general impact of  $\text{SO}_2$  was moderate on Cu/BEA and much less pronounced than on Cu/SSZ-13 despite the greater  $\text{SO}_2$  storage of Cu/BEA (Table 1). One possible reason for this could be that since BEA has significantly larger pores, the adsorbed sulfur species causes less sterical hindrance for the reactants to access the Cu sites. Like for Cu/SSZ-13,  $\text{SO}_3$  poisoning was more detrimental than  $\text{SO}_2$  poisoning on Cu/BEA. The  $\text{SO}_3$ -poisoned Cu/BEA was again more active than the  $\text{SO}_3$ -poisoned Cu/SSZ-13 with 86% NO conversion at 300 °C, compared with 44% for Cu/SSZ-13.

### 3.3 Fast SCR Activity for Degreened and Poisoned Samples

The selective reduction of an equimolar mixture of NO and  $\text{NO}_2$  with  $\text{NH}_3$  in presence of  $\text{O}_2$  is known as fast SCR due to its faster kinetics. These conditions are aimed by the upstream oxidation catalyst which converts NO to  $\text{NO}_2$  for a more efficient  $\text{NO}_x$  removal process. However, at a high temperature, this catalyst also converts  $\text{SO}_2$  to  $\text{SO}_3$ . The fast SCR reaction was studied, and the activity is reported in Fig. 6 for Cu/SSZ-13 (a) and Cu/BEA (b). The NO conversion of the degreened Cu/SSZ-13 was close to 80% at 175 °C and increased to higher than 90% between 200 and 400 °C. The activity declined below 80% at 500 °C. Similar observations can be made for Cu/BEA as seen in Fig. 6. It can be noted that the NO conversion at low temperature

was higher for the fast SCR than for the standard SCR. The  $\text{NO}_2$  conversion (not shown) was high (above 90% and for mid-range temperatures 100%). The  $\text{SO}_2$  exposure led to a significant activity decrease of Cu/SSZ-13 below 200 °C. However, the fast SCR was less impaired than the standard SCR. The  $\text{SO}_3$  poisoning led to an even greater deactivation of Cu/SSZ-13 with a maximum NO conversion of only 80% at 300 °C. As opposed to Cu/SSZ-13, Cu/BEA was only mildly deactivated by  $\text{SO}_2$  and  $\text{SO}_3$  exposure (Fig. 6b). The lowest conversion for Cu/BEA, noted at 175 °C, was 65% and 82% after  $\text{SO}_2$  poisoning and  $\text{SO}_3$  poisoning, respectively. It appeared clearly that Cu/SSZ-13 is more sensitive than Cu/BEA to both  $\text{SO}_2$  and  $\text{SO}_3$  exposure. Cu/SSZ-13 is prone to severe deactivation when exposed to sulfur compounds, especially  $\text{SO}_3$ . BEA is a type of zeolite characterized by wide channels constituted of 12-membered rings interconnected and forming cages [29]. SSZ-13, on the other hand, is a narrow-pore zeolite which consists of 6-membered rings forming hexagonal prisms (d6r) and chabazite cages (cha). The widest window of the chabazite cages is made of 8-membered rings with a 3.8 Å diameter. The smaller channel opening and cage volume could be one reason why Cu/SSZ-13 is more prone to pore blocking by sulfate species than BEA and more subjected to deactivation by  $\text{SO}_2$  and  $\text{SO}_3$ . Cu/SSZ-13 is preferred as an SCR catalyst for its better hydrothermal stability and lower hydrocarbon storage than Cu/BEA. However, our results show that SSZ-13 is more subjected to sulfur-induced deactivation than Cu/BEA. Since  $\text{SO}_3$  has a much larger effect than  $\text{SO}_2$  on Cu/SSZ-13, it would be beneficial to produce as little  $\text{SO}_3$  as possible. For a durable and optimal  $\text{NO}_x$  reduction, it is crucial to operate

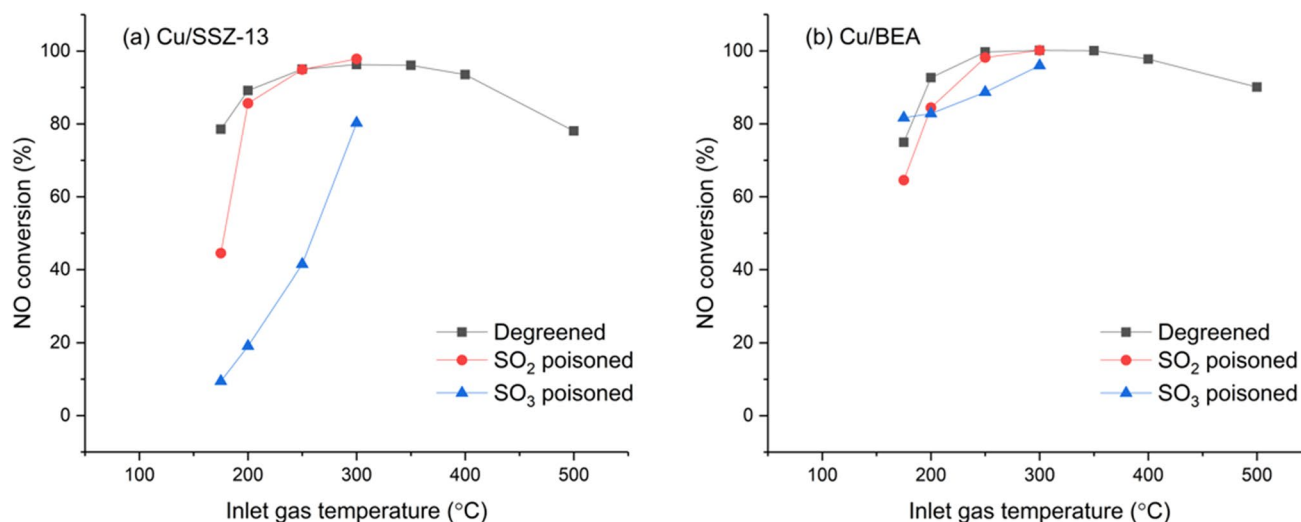


**Fig. 6** Fast SCR activity (NO conversion) of degreened,  $\text{SO}_2$ -poisoned, and  $\text{SO}_3$ -poisoned **a** Cu/SSZ-13 and **b** Cu/BEA. Feed: 200 ppm NO, 200 ppm  $\text{NO}_2$ , 400 ppm  $\text{NH}_3$ , 8%  $\text{O}_2$ , 5%  $\text{H}_2\text{O}$  in Ar, flowrate=1.2L/min. Note: only NO conversion is shown, the  $\text{NO}_2$

conversion was 100% at all temperature steps. During  $\text{SO}_2$  poisoning, 30 ppm  $\text{SO}_2$  was used, and during  $\text{SO}_3$  poisoning, 24 ppm  $\text{SO}_3$  and 6 ppm  $\text{SO}_2$ , in the presence of 400 ppm NO, 8%  $\text{O}_2$ , 5%  $\text{H}_2\text{O}$  for both cases

in fast SCR conditions since Cu/SSZ-13 is less sensitive to  $\text{SO}_2$  and  $\text{SO}_3$  in fast SCR conditions than in standard SCR conditions.

The impact of  $\text{SO}_2$  exposure on fast SCR activity is moderate compared to its impact on standard SCR when the SCR unit is considered. However, taking the whole aftertreatment system into account that consists of an oxidation catalyst followed by the SCR converter,  $\text{SO}_2$  will affect the oxidation catalyst and inhibit its ability to oxidize NO to  $\text{NO}_2$  [14] which is necessary to perform the fast SCR on the SCR catalyst. Overall,  $\text{SO}_2$  exposure will decrease the  $\text{NO}_2/\text{NO}_x$  ratio which will lower the amount of  $\text{NO}_x$  that can react in the fast SCR reaction. This will lead to an overall lower rate since a higher amount of NO needs to react in the slower standard SCR reaction.

### 3.4 Regeneration in SCR Conditions: Standard SCR

To desorb sulfur and restore the initial activity, hydrothermal treatment at a high temperature is usually advocated [9, 19]. A reductive atmosphere is also beneficial to decompose the stored sulfur oxides [30]. However, such treatments affect the zeolite structure and the dispersion of active copper centers. High temperature in presence of water vapor is known to degrade the crystallinity of the zeolite structure, and at very high temperatures, the structure collapses [2, 31], which urges the development of highly stable zeolites. The detrimental effect of reducing treatment on the copper dispersion and the subsequent SCR activity has been revealed by Auvray et al. [6, 32]. It was shown that exchanged copper ions tend to agglomerate in larger particles under the

action of hydrogen. Therefore, in this study, the regeneration in lean SCR conditions at temperatures up to 500 °C was investigated. The stepwise activity measurement for standard and fast SCR was used and repeated after sulfur poisoning as a regeneration procedure. Each time the standard SCR activity was measured, the upper temperature boundary was increased from 300 °C for the first measurement after poisoning to 400 and 500 °C for the second and third measurements, respectively. Figure 7 presents the standard SCR activity of Cu/SSZ-13 (a) and Cu/BEA (b) after  $\text{SO}_2$  poisoning and regeneration in standard SCR conditions. For Cu/SSZ-13 (Fig. 7a), the NO conversion measured during the first repetition (denoted regeneration 2) was similar to the NO conversion measured after  $\text{SO}_2$  poisoning (denoted regeneration 1). Since the maximum temperature of the regeneration 1 stage was 300 °C, this result indicates that no regeneration occurred in SCR conditions at 300 °C. However, a significant NO conversion improvement was noted for the second measurement repetition (regeneration 3) between 200 and 300 °C. Before the regeneration 3 experiment, the poisoned catalyst was exposed to SCR conditions at 400 °C during the regeneration 2. This result shows that partial regeneration of  $\text{SO}_2$ -poisoned Cu/SSZ-13 occurred under SCR conditions at 400 °C.

The NO conversion was also improved by the poisoning and regeneration compared to the degreened one at temperatures higher than 350 °C. This has also been found for thermal aging [33] and could be due to larger deactivation of the ammonia oxidation reaction resulting in increased selectivity for the SCR reaction. The presence of SCR conditions is important for the sulfur regeneration, as previously

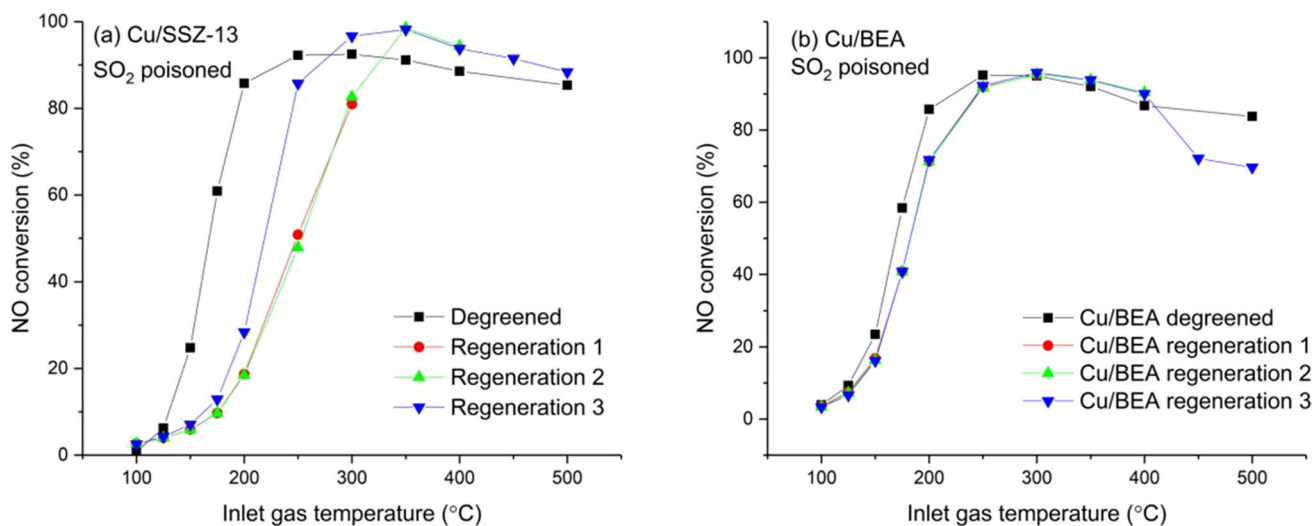


**Fig. 7** Standard SCR activity (NO conversion) of degreened catalysts and during regeneration of  $\text{SO}_2$ -poisoned **a** Cu/SSZ-13 and **b** Cu/BEA. Feed: 400 ppm NO, 400 ppm  $\text{NH}_3$ , 8%  $\text{O}_2$ , 5%  $\text{H}_2\text{O}$  in Ar, flowrate = 1.2 L/min. Regeneration 1 is performed directly after the

poisoning, thus showing the poisoned catalyst. Note that regeneration 1 and 2 for Cu/SSZ-13 and regeneration 1, 2, and 3 for Cu/BEA are overlapping. During  $\text{SO}_2$  poisoning, 30 ppm  $\text{SO}_2$  was used in the presence of 400 ppm NO, 8%  $\text{O}_2$ , 5%  $\text{H}_2\text{O}$

shown by Kumar et al. [30]. Moreover, Brookshear et al. [8] reported significant regeneration in lean conditions at 350 °C but obtained full activity recovery only with a DeSO<sub>x</sub> temperature of 500 °C. Hammershøi et al. [19] found almost full recovery after regeneration in SCR conditions at 550 °C. However, some remaining poisoning was still found after the 550 °C treatment in that study.

Sulfur poisoning and regeneration for Cu/BEA are shown in Fig. 7b. The results show that Cu/BEA was much less influenced by SO<sub>2</sub> poisoning compared to Cu/SSZ-13, but also that the Cu/BEA did not regain any activity during the regenerations up to 400 °C. This result can indicate an irreversible deactivation caused by the SO<sub>2</sub> poisoning to the catalyst or that higher temperatures are needed for the regeneration.

The effect of the regeneration of SO<sub>3</sub>-poisoned catalysts is shown in Fig. 8. Like after SO<sub>2</sub> poisoning, the activity of Cu/SSZ-13 (Fig. 8a) was not recovered at all during the regeneration 2 (after SCR conditions up to 300 °C in regeneration 1) but was improved during the regeneration 3. This indicates that partial regeneration of a SO<sub>3</sub>-poisoned Cu/SSZ-13 was possible at 400 °C. Like after SO<sub>2</sub> poisoning, the NO conversion at high temperatures (> 350 °C) was improved by the SO<sub>3</sub>/SO<sub>2</sub> poisoning and the regeneration. After regeneration 3, the standard SCR activity of Cu/SSZ-13 was significantly lower when the poisoning was carried out with the SO<sub>3</sub>/SO<sub>2</sub> mixture than with SO<sub>2</sub>.

The SO<sub>3</sub> poisoning impaired significantly the activity of Cu/BEA. In these conditions, the regeneration had a greater impact than on the SO<sub>2</sub>-poisoned Cu/BEA. Figure 8b shows the partial activity recovery during regeneration 3, indicating

that SCR conditions at 400 °C were able to partly reactivate Cu/BEA. This observation is similar for both Cu/SSZ-13 and Cu/BEA after SO<sub>3</sub>/SO<sub>2</sub> poisoning.

### 3.5 Regeneration in SCR Conditions: Fast SCR

The various sulfur species formed on the catalyst have different stability and affect different sites. The exchanged Cu attached to one Al center (ZCuOH) was reported to be strongly affected upon sulfation of Cu/SSZ-13 [34]. Jangjou et al. [28] suggested that copper bisulfites form preferentially on ZCuOH while ammonium sulfates tend to form on Cu<sup>2+</sup> connected to a pair of framework Al (Z2Cu sites). These two sites present different reactivity and roles in oxidation reactions and SCR. Therefore, the impact of sulfation and regeneration on the fast SCR was studied. Fast SCR activity measurements were part of the regeneration procedure (see Fig. 1). However, since full conversion of NO<sub>x</sub> was reached at a rather low temperature, the measurements were limited to 300 °C. Consequently, the impact of the fast SCR sequences on the sulfur regeneration was expected to be minor compared to the standard SCR steps. The fast SCR activity was measured four times after poisoning. It allowed us to probe the regeneration after each standard SCR step, whose maximum temperature was 300, 400, and 500 °C, respectively. Figure 9 shows the NO conversion during fast SCR of the SO<sub>2</sub>-poisoned Cu/SSZ-13 (a) and Cu/BEA (b). Figure 9a shows that regeneration 1 and 2 were similar for Cu/SSZ-13, indicating no regeneration during SCR at 300 °C. However, fast SCR activity was regained during SCR at 400 and 500 °C, as suggested by the regeneration 3

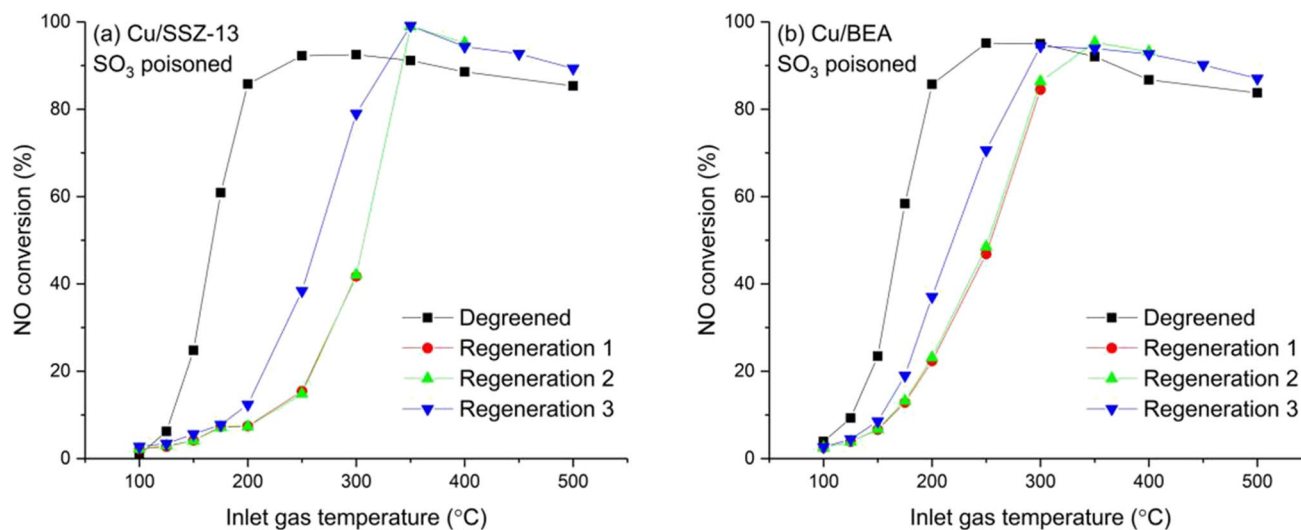


**Fig. 8** Standard SCR activity (NO conversion) of degreened catalysts and during regeneration of SO<sub>3</sub>-poisoned **a** Cu/SSZ-13 and **b** Cu/BEA. Feed: 400 ppm NO, 400 ppm NH<sub>3</sub>, 8% O<sub>2</sub>, 5% H<sub>2</sub>O in Ar, flowrate=1.2L/min. Regeneration 1 is performed directly after the

poisoning, thus showing the poisoned catalyst. During SO<sub>3</sub> poisoning, 24 ppm SO<sub>3</sub> and 6 ppm SO<sub>2</sub>, in the presence of 400 ppm NO, 8% O<sub>2</sub>, 5% H<sub>2</sub>O were used

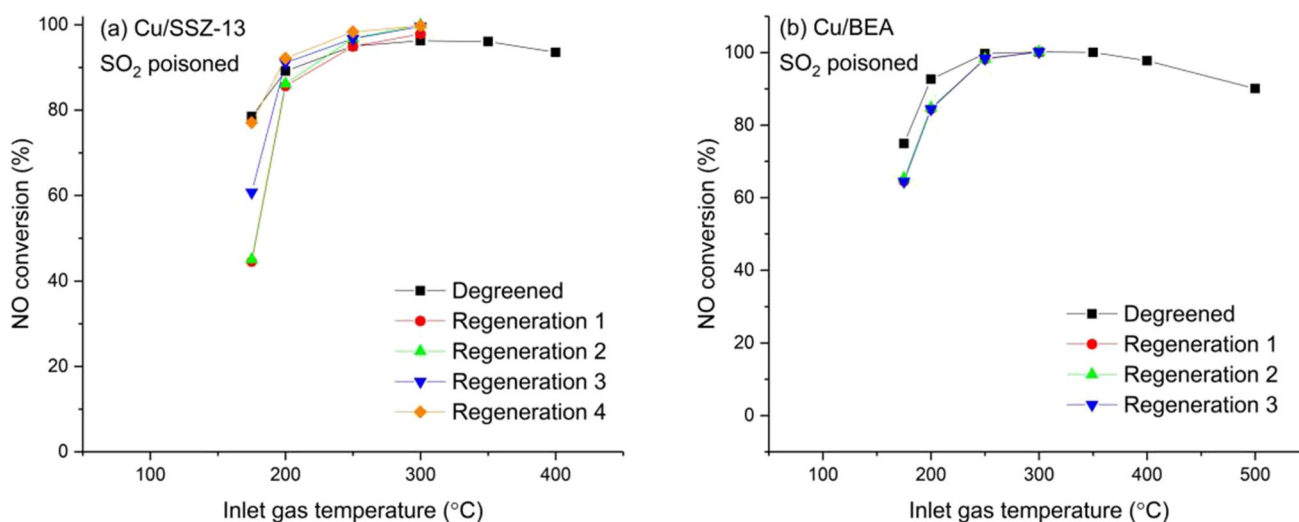


**Fig. 9** Fast SCR activity (NO conversion) of degreened catalysts and during regeneration of SO<sub>2</sub>-poisoned **a** Cu/SSZ-13 and **b** Cu/BEA. Feed: 200 ppm NO, 200 ppm NO<sub>2</sub>, 400 ppm NH<sub>3</sub>, 8% O<sub>2</sub>, 5% H<sub>2</sub>O

and regeneration 4 measurements. The full activity recovery at 175 °C can be noted during regeneration 4. The improvement of the degreened activity can be noted as well between 200 and 300 °C. As for the standard SCR, the regeneration up to 400 °C was inefficient for the fast SCR on Cu/BEA (Fig. 9b) after SO<sub>2</sub> poisoning; however, Cu/BEA was also significantly less poisoned compared to Cu/SSZ-13.

The regeneration effect after SO<sub>3</sub>/SO<sub>2</sub> poisoning was then examined for the fast SCR (Fig. 10). SO<sub>3</sub> greatly decreased the fast SCR activity of Cu/SSZ-13 (Fig. 10a), but regeneration was possible in SCR conditions at 400 and 500 °C,

in Ar, flowrate=1.2L/min. Regeneration 1 is standard SCR up to 300 °C. During SO<sub>2</sub> poisoning, 30 ppm SO<sub>2</sub> was used in the presence of 400 ppm NO, 8% O<sub>2</sub>, 5% H<sub>2</sub>O

whereas 300 °C was not sufficient to observe any improvement. After regeneration 4, full recovery was not obtained at 175 °C, indicating that some sulfur was remaining on the catalyst. Interestingly, the activity was greater than the degreened activity at a temperature between 200 and 300 °C. Sulfur poisoning results in the formation of different sulfur species such as H<sub>2</sub>SO<sub>4</sub>, CuSO<sub>4</sub>, Al<sub>2</sub>(SO<sub>4</sub>)<sub>3</sub> [4], and also ammonium sulfates (in the presence of ammonia). During mild regeneration, such as our regeneration, it is likely that some of the ammonium sulfates, which are less stable [12], are decomposed, while the more stable copper sulfates

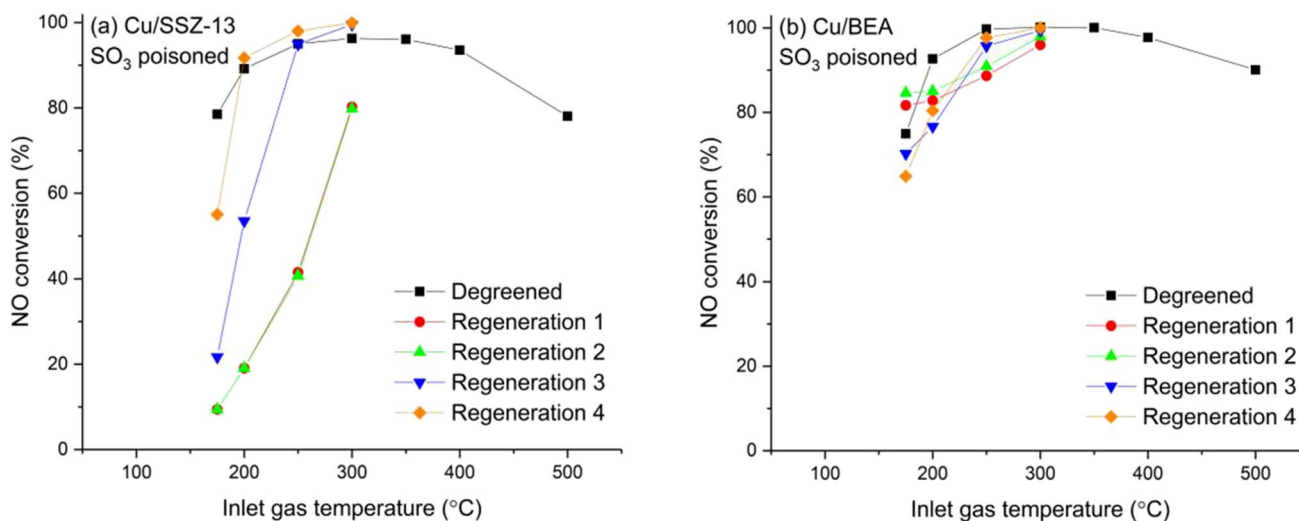


**Fig. 10** Fast SCR activity (NO conversion) of degreened catalysts and during regeneration of SO<sub>3</sub>-poisoned **a** Cu/SSZ-13 and **b** Cu/BEA. Feed: 200 ppm NO, 200 ppm NO<sub>2</sub>, 400 ppm NH<sub>3</sub>, 8% O<sub>2</sub>, 5%

H<sub>2</sub>O in Ar, flowrate=1.2L/min. Regeneration 1 is standard SCR up to 300 °C. During SO<sub>3</sub> poisoning, 24 ppm SO<sub>3</sub> and 6 ppm SO<sub>2</sub> were used in the presence of 400 ppm NO, 8% O<sub>2</sub>, 5% H<sub>2</sub>O for both cases



remain. The formation of copper sulfates is increased in the presence of copper oxides [12], and copper oxides also enhance the ammonia oxidation. It is possible that the presence of copper sulfates reduces the competitive ammonia oxidation reaction and thereby increases the selectivity in the SCR process. Separate ammonia oxidation experiments (data not shown) show that some ammonia oxidation occurs at 300 °C, which could explain the increased SCR activity at 300 °C, but not at 200 °C. However, the N<sub>2</sub>O formation also decreased significantly during poisoning (data not shown), indicating that there is less ammonium nitrate formation after sulfur poisoning. Since ammonium nitrate formation hinders the SCR activity [35], we suggest that the reason for the increased SCR activity at low temperature could be related to that sulfur species blocks the ammonium nitrate formation, and thereby results in increased NO conversion. The SO<sub>3</sub>/SO<sub>2</sub> exposure on Cu/BEA (Fig. 10b) had a dual effect with a promotion at 175 °C and poisoning at a higher temperature. These two features of the poisoned Cu/BEA tended to disappear with the regeneration. Figure 10b displays the global improvement during regeneration 2 and the degradation of the activity at 175 °C in regeneration 3 and 4. At the end of the process, however, the activity at 250 and 300 °C had retrieved its degreened level.

In general, Cu/SSZ-13 was more affected by SO<sub>2</sub> and SO<sub>3</sub>/SO<sub>2</sub> poisoning than Cu/BEA. This was clearly evidenced with SO<sub>2</sub> poisoning since it only decreased moderately the SCR activity of Cu/BEA. However, in real conditions, SO<sub>3</sub> is formed over the diesel oxidation catalyst and our results demonstrated that SO<sub>3</sub> had a greater impact than SO<sub>2</sub> on both Cu/SSZ-13 and Cu/BEA. SO<sub>3</sub> exposure was able to decrease significantly the standard SCR of the SO<sub>2</sub>-resistant Cu/BEA and the fast SCR activity of Cu/

SSZ-13. Our results suggest the importance of adding SO<sub>3</sub> during poisoning studies of SCR catalysts and in addition that the zeolite used plays a major role in the poisoning and regeneration. These results emphasize the need to study in detail the SO<sub>3</sub> chemistry on the SCR catalysts. The regeneration in SCR operating conditions was possible to some extent whether the poisoning was performed using SO<sub>2</sub> or SO<sub>3</sub>/SO<sub>2</sub>, which indicates the chemical and reversible nature of the poisoning.

### 3.6 DRIFT Spectroscopy

NO adsorption was performed on degreened and SO<sub>2</sub>-poisoned catalysts in a DRIFT cell. Figure 11 compares the FTIR spectra recorded after 55 min of NO exposure on Cu/SSZ-13 and Cu/BEA. On Cu/SSZ-13, the T-O-T structure vibration is disturbed by the exchanged Cu<sup>2+</sup>. Upon adsorption of a probe molecule such as NO or NH<sub>3</sub> on Cu, the T-O-T vibration bands appear as negative bands at approximately 900 cm<sup>-1</sup> and 950 cm<sup>-1</sup>. These bands are known to correspond to the Z2Cu and ZCuOH centers, respectively [11]. The inset of Fig. 11a shows that the ratio ZCuOH/Z2Cu was lower on the sulfated Cu/SSZ-13 than the degreened sample. These results indicate that stable sulfates were formed preferentially on the copper coordinated to one framework Al and one hydroxyl group (ZCuOH). Thus, a part of these ZCuOH sites was blocked and unavailable to NO during the NO adsorption step. The decrease of the amount of ZCuOH upon sulfation was also observed by Tang et al. [20] and Luo et al. [34]. Shih et al. [3] reported on the higher S:Cu molar ratio of ZCuOH than Z2Cu sites indicating that ZCuOH was more prone to sulfation whereas Z2Cu was rather insensitive to SO<sub>2</sub> poisoning, which is in

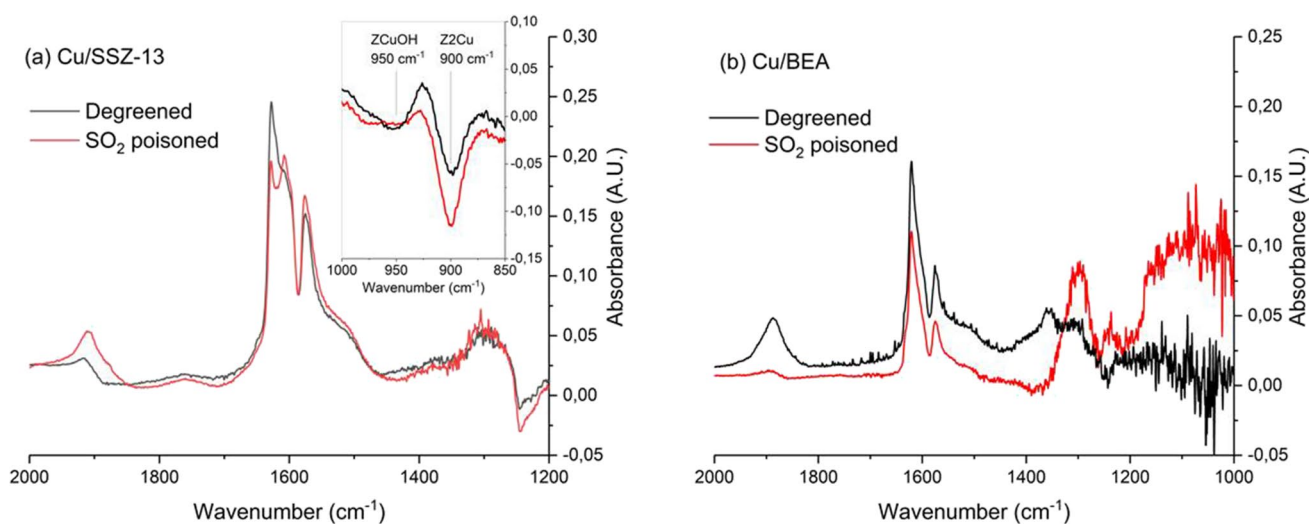


**Fig. 11** DRIFT spectroscopy absorbance spectra of NO at 30 °C after oxidizing pretreatment at 500 °C of degreened and SO<sub>2</sub>-poisoned **a** Cu/SSZ-13 and **b** Cu/BEA catalysts. The spectra were recorded after 55 min of NO exposure



line with our results. ZCuOH can readily form stable copper bisulfites and bisulfates in the presence of SO<sub>2</sub> alone while the sulfation of Z2Cu sites is obtained with cofeeding SO<sub>2</sub> and NH<sub>3</sub> to form ammonium sulfates [36]. Catalysts with a high Si:Al ratio present a higher ZCuOH:Z2Cu and therefore are prone to formation of stable copper bisulfites that oxidize further to bisulfates. Catalysts with low Si:Al are mainly deactivated by ammonium sulfates. Low-temperature deactivation occurs on Cu/SSZ-13 upon SO<sub>2</sub> poisoning regardless of the Si:Al ratio. However, the regeneration is greatly impacted by the nature of the inhibiting sulfate species. Therefore, regeneration of low Si:Al Cu/SSZ-13 can be achieved at relatively low temperature. Upon hydrothermal aging, Cu cations migrate through the CHA framework and it has been evidenced that ZCuOH is converted to the more stable Z2Cu [20, 23, 34] located in the 6-member rings. In particular, Wei et al. [37] have demonstrated a decrease in sulfur storage and the mitigation of SO<sub>2</sub> poisoning on mildly hydrothermally aged (750 °C) Cu/SSZ-13. The conversion of ZCuOH to Z2Cu offers a greater resistance to SO<sub>2</sub> poisoning and an improved SCR efficiency at high temperature because ZCuOH is active for NH<sub>3</sub> oxidation. However, the SCR activity is lost at low temperature, which is very problematic. After higher hydrothermal aging temperature (800 °C), Wijayanti et al. [12] also found a lower sulfur amount stored on the Cu/SSZ-13, but the formation of some copper oxides resulted in more stable copper sulfates being formed. In addition, copper oxides are less active for ammonia SCR reaction, which would reduce the catalyst efficiency.

The band at 1910 cm<sup>-1</sup> could be assigned to NO adsorbed on Cu<sup>2+</sup> (mononitrosyl group) [38–40]. It increased rapidly before decreasing slowly with time on the poisoned Cu/SSZ-13. The band at 1580 cm<sup>-1</sup> can be assigned to a nitrate species adsorbed on Cu [38] while the bands at 1607 and 1628 cm<sup>-1</sup> can be assigned to monodentate and bridging nitrates adsorbed on the zeolite framework, respectively [41]. SO<sub>2</sub> poisoning affected these latter two bands by switching their relative ratio, increasing the monodentate/bridged nitrate ratio. This result was consistent with the blocking of sites by sulfates since bridge nitrates required two sites.

NO adsorption on Cu/BEA showed similarities with Cu/SSZ-13 (Fig. 11b) concerning the monodentate nitrate band at 1619 cm<sup>-1</sup> and the nitrate on Cu<sup>2+</sup> band at 1575 cm<sup>-1</sup>. The band assigned to NO adsorbed on Cu<sup>2+</sup> was located at 1890 cm<sup>-1</sup> on Cu/BEA. This band decreased rapidly when NO was turned off while the band at 1350 cm<sup>-1</sup> kept growing. The latter band was tentatively assigned to nitrite species. On the poisoned Cu/BEA, the NO-Cu<sup>2+</sup> band decreased during NO exposure after 30 min. In addition, new bands at 1320 cm<sup>-1</sup> and 1240 cm<sup>-1</sup> and a broad band at 1100 cm<sup>-1</sup> appeared. The bands at 1320 and 1240 cm<sup>-1</sup>

are tentatively assigned to different kinds of nitrates, which were more likely to form than nitrites on an oxidized surface. Negri et al. [42] observed a band at 1310 cm<sup>-1</sup> during NO adsorption at 50 °C on Cu-CHA that they assigned to a type of monodentate chelating nitrate on Cu. The broad band at 1100 cm<sup>-1</sup> is in the spectral region of sulfates [43–45]. This result suggests the conversion of sulfate species during NO adsorption on SO<sub>2</sub>-poisoned Cu/BEA. The growth of this sulfate species can be due to the mobility of a different sulfate species or the interaction with the adsorbed NO. This was not observed on poisoned Cu/SSZ-13 which indicates the more difficult reactivity and/or mobility of the sulfate species on Cu/SSZ-13 than on Cu/BEA. This result agrees with the activity measured after SO<sub>2</sub> poisoning which showed a great negative impact on Cu/SSZ-13 and only a moderate activity loss on Cu/BEA.

## 4 Conclusions

The poisoning of Cu/BEA and Cu/SSZ-13 with SO<sub>2</sub> and a mixture of SO<sub>3</sub> and SO<sub>2</sub> (SO<sub>3</sub>:SO<sub>2</sub>=4) was studied on washcoated monoliths. After a degreening, Cu/SSZ-13 and Cu/BEA showed similar SCR activities. It should be noted that Cu/BEA is not commercially applicable and is used to compare with Cu/SSZ-13 for mechanistic reasons. The XRD analysis showed that the structure of the zeolites was not damaged by sulfur treatment. XRD analysis did not detect any large Cu particles either, which confirmed the absence of structural damages. The number and strength of acidic sites, determined by NH<sub>3</sub>-TPD, were not strongly affected after poisoning and subsequent regeneration. Several regeneration treatments in SCR conditions were attempted in order to measure the degree of recovery.

There are both similarities and differences between the poisoning and regeneration of Cu/SSZ-13 and Cu/BEA. Firstly, both catalysts exhibited a decreased standard SCR activity after poisoning by SO<sub>2</sub>; however, Cu/SSZ-13 was significantly more deactivated. Interestingly, the Cu/BEA contained more adsorbed sulfur after poisoning compared to Cu/SSZ-13. These results indicate that even though there were more sulfur available in Cu/BEA, it did not affect the activity equally much. One possible reason for this could be that the Cu/BEA has significantly larger pores, so there could be less sterical hindrance by the sulfur addition. Moreover, the deactivation noted after SO<sub>3</sub>/SO<sub>2</sub> poisoning was much more intense for both catalysts. Cu/BEA, however, was again less poisoned compared to Cu/SSZ-13.

Evaluation of standard SCR after regeneration revealed that 300 °C was not enough to regain any activity, while some regeneration was found for Cu/SSZ-13 after regeneration at 400 °C. It should be noted that no regeneration was observed for this condition for Cu/BEA, but on the other

hand, it was only mildly poisoned. SO<sub>3</sub> poisoning was much more severe for both catalysts, but especially Cu/SSZ-13. Both catalysts now exhibited some regeneration capabilities in SCR conditions at 400 °C. Examining the fast SCR after different regenerations in standard SCR after SO<sub>2</sub> poisoning showed that Cu/SSZ-13 could regain its full activity after regeneration at 500 °C. After SO<sub>3</sub> poisoning, much of the fast SCR activity was regained for both catalysts after 500 °C regeneration, but not all. Both catalysts exhibited less activity after SO<sub>3</sub> poisoning and regeneration compared with fresh catalysts.

DRIFT spectroscopy revealed the interaction between sulfates and the ZCuOH sites of Cu/SSZ-13 which can explain the strong deactivation by blocking the active sites. Moreover, Cu/BEA showed clear sulfate bands in DRIFT, which is consistent with the large amount of stored sulfur species by ICP measurements.

**Funding** We received the financial support from the Swedish Research Council [Grant number 642–2014–5733].

## Declarations

**Conflict of Interest** The authors declare that they have no competing interests.

**Open Access** This article is licensed under a Creative Commons Attribution 4.0 International License, which permits use, sharing, adaptation, distribution and reproduction in any medium or format, as long as you give appropriate credit to the original author(s) and the source, provide a link to the Creative Commons licence, and indicate if changes were made. The images or other third party material in this article are included in the article's Creative Commons licence, unless indicated otherwise in a credit line to the material. If material is not included in the article's Creative Commons licence and your intended use is not permitted by statutory regulation or exceeds the permitted use, you will need to obtain permission directly from the copyright holder. To view a copy of this licence, visit <http://creativecommons.org/licenses/by/4.0/>.

## References

- Olsson, L., Wijayanti, K., Leistner, K., Kumar, A., Joshi, S.Y., Kamasamudram, K., Currier, N.W., Yezerets, A.: A kinetic model for sulfur poisoning and regeneration of Cu/SSZ-13 used for NH<sub>3</sub>-SCR. *Appl. Catal. B Environ.* **183**, 394–406 (2016)
- Shan, Y., Shi, X., Yan, Z., Liu, J., Yu, Y., He, H.: Deactivation of Cu-SSZ-13 in the presence of SO<sub>2</sub> during hydrothermal aging. *Catal. Today* **320**, 84–90 (2019)
- Shih, A.J., Khurana, I., Li, H., González, J., Kumar, A., Paolucci, C., Lardinois, T.M., Jones, C.B., Albarracín Caballero, J.D., Kamasamudram, K., Yezerets, A., Delgass, W.N., Miller, J.T., Villa, A.L., Schneider, W.F., Gounder, R., Ribeiro, F.H.: Spectroscopic and kinetic responses of Cu-SSZ-13 to SO<sub>2</sub> exposure and implications for NO<sub>x</sub> selective catalytic reduction. *Appl. Catal. A Gen.* **574**, 122–131 (2019)
- Su, W., Li, Z., Zhang, Y., Meng, C., Li, J.: Identification of sulfate species and their influence on SCR performance of Cu/CHA catalyst, *Catalysis. Sci. Technol.* **7**, 1523–1528 (2017)
- Wijayanti, K., Leistner, K., Chand, S., Kumar, A., Kamasamudram, K., Currier, N.W., Yezerets, A., Olsson, L.: Deactivation of Cu-SSZ-13 by SO<sub>2</sub> exposure under SCR conditions, *Catalysis. Sci. Technol.* **6**, 2565–2579 (2016)
- Auvray, X., Grant, A., Lundberg, B., Olsson, L.: Lean and rich aging of a Cu/SSZ-13 catalyst for combined lean NO<sub>x</sub> trap (LNT) and selective catalytic reduction (SCR) concept, *Cat. Sci. Technol.* **9**, 2152–2162, (2019)
- Bergman, S.L., Dahlin, S., Mesilov, V.V., Xiao, Y., Englund, J., Xi, S., Tang, C., Skoglundh, M., Pettersson, L.J., Bernasek, S.L.: In-situ studies of oxidation/reduction of copper in Cu-CHA SCR catalysts: comparison of fresh and SO<sub>2</sub>-poisoned catalysts, *Appl. Catal. B Environ.* **269**, 118722, (2020)
- Brookshear, D.W., Nam, J.G., Nguyen, K., Toops, T.J., Binder, A.: Impact of sulfation and desulfation on NO<sub>x</sub> reduction using Cu-chabazite SCR catalysts. *Catal. Today* **258**, 359–366 (2015)
- Dahlin, S., Lantto, C., Englund, J., Westerberg, B., Regali, F., Skoglundh, M., Pettersson, L.J.: Chemical aging of Cu-SSZ-13 SCR catalysts for heavy-duty vehicles – influence of sulfur dioxide. *Catal. Today* **320**, 72–83 (2019)
- Jangjou, Y., Ali, M., Chang, Q., Wang, D., Li, J., Kumar, A., Epling, W.S.: Effect of SO<sub>2</sub> on NH<sub>3</sub> oxidation over a Cu-SAPO-34 SCR catalyst, *Catalysis. Sci. Technol.* **6**, 2679–2685 (2016)
- Wang, A., Olsson, L.: Insight into the SO<sub>2</sub> poisoning mechanism for NO<sub>x</sub> removal by NH<sub>3</sub>-SCR over Cu/LTA and Cu/SSZ-13, *Chem. Eng. J.* **395**, 125048 (2020)
- Wijayanti, K., Xie, K., Kumar, A., Kamasamudram, K., Olsson, L.: Effect of gas compositions on SO<sub>2</sub> poisoning over Cu/SSZ-13 used for NH<sub>3</sub>-SCR. *Appl. Catal. B Environ.* **219**, 142–154 (2017)
- Auvray, X., Pingel, T., Olsson, E., Olsson, L.: The effect gas composition during thermal aging on the dispersion and NO oxidation activity over Pt/Al<sub>2</sub>O<sub>3</sub> catalysts. *Appl. Catal. B Environ.* **129**, 517–527 (2013)
- Auvray, X.P., Olsson, L.: Sulfur dioxide exposure: a way to improve the oxidation catalyst performance. *Ind. Eng. Chem. Res.* **52**, 14556–14566 (2013)
- Koutsopoulos, S., Rasmussen, S.B., Eriksen, K.M., Fehrmann, R.: The role of support and promoter on the oxidation of sulfur dioxide using platinum based catalysts. *Appl. Catal. A Gen.* **306**, 142–148 (2006)
- Xue, E., Seshan, K., Ross, J.R.H.: Roles of supports, Pt loading and Pt dispersion in the oxidation of NO to NO<sub>2</sub> and of SO<sub>2</sub> to SO<sub>3</sub>. *Appl. Catal. B Environ.* **11**, 65–79 (1996)
- Kumar, A., Smith, M.A., Kamasamudram, K., Currier, N.W., An, H., Yezerets, A.: Impact of different forms of feed sulfur on small-pore Cu-zeolite SCR catalyst. *Catal. Today* **231**, 75–82 (2014)
- Cheng, Y., Montreuil, C., Cavataio, G., and Lambert, C., The Effects of SO<sub>2</sub> and SO<sub>3</sub> Poisoning on Cu/Zeolite SCR Catalysts, SAE Technical Paper 2009-01-0898, (2009)
- Hammershøi, P.S., Jangjou, Y., Epling, W.S., Jensen, A.D., Janssens, T.V.W.: Reversible and irreversible deactivation of Cu-CHA NH<sub>3</sub>-SCR catalysts by SO<sub>2</sub> and SO<sub>3</sub>. *Appl. Catal. B Environ.* **226**, 38–45 (2018)
- Tang, Y.D., Wang, D., Wang, X., Zha, Y.H., An, H.M., Kamasamudram, K., Yezerets, A.: Impact of low temperature sulfur exposure on the aging of small pore Cu-zeolite SCR catalyst. *Catal. Today* **360**, 234–240 (2021)
- Paolucci, C., Khurana, I., Parekh, A.A., Li, S.C., Shih, A.J., Li, H., Di Iorio, J.R., Albarracín-Caballero, J.D., Yezerets, A., Miller, J.T., Delgass, W.N., Ribeiro, F.H., Schneider, W.F., Gounder, R.: Dynamic multinuclear sites formed by mobilized copper ions in NO<sub>x</sub> selective catalytic reduction. *Science* **357**, 898–903 (2017)

22. Wilken, N., Wijayanti, K., Kamasamudram, K., Currier, N.W., Vedaiyan, R., Yezerets, A., Olsson, L.: Mechanistic investigation of hydrothermal aging of Cu-beta for ammonia SCR. *Appl. Catal. B Environ.* **111**, 58 (2012)
23. Luo, J.Y., Oh, H., Henry, C., Epling, W.: Effect of C<sub>3</sub>H<sub>6</sub> on selective catalytic reduction of NO<sub>x</sub> by NH<sub>3</sub> over a Cu/zeolite catalyst: a mechanistic study. *Appl. Catal. B Environ.* **123**, 296–305 (2012)
24. Blakeman, P.G., Burkholder, E.M., Chen, H.Y., Collier, J.E., Fedeyko, J.M., Jobson, H., Rajaram, R.R.: The role of pore size on the thermal stability of zeolite supported Cu SCR catalysts. *Catal. Today* **231**, 56–63 (2014)
25. Valtchev, V., Rigolet, S., Bozhilov, K.N.: Gel evolution in a FAU-type zeolite yielding system at 90 degrees C. *Microporous Mesoporous Mater.* **101**, 73–82 (2007)
26. Luo, J., Gao, F., Kamasamudram, K., Currier, N., Peden, C.H.F., Yezerets, A.: New insights into Cu/SSZ-13 SCR catalyst acidity. Part I: Nature of acidic sites probed by NH<sub>3</sub> titration. *J. Catal.* **348**, 291–299 (2017)
27. Leistner, K., Xie, K., Kumar, A., Kamasamudram, K., Olsson, L.: Ammonia desorption peaks can be assigned to different copper sites in Cu/SSZ-13. *Catal. Lett.* **147**, 1882–1890 (2017)
28. Jangjou, Y., Sampara, C.S., Gu, Y., Wang, D., Kumar, A., Li, J., Epling, W.S.: Mechanism-based kinetic modeling of Cu-SSZ-13 sulfation and desulfation for NH<sub>3</sub>-SCR applications. *React. Chem. Eng.* **4**, 1038–1049 (2019)
29. Treacy, M.M.J., Newsam, J.M.: Two new three-dimensional twelve-ring zeolite frameworks of which zeolite beta is a disordered intergrowth. *Nature* **332**, 249–251 (1988)
30. Kumar, A., Smith, M.A., Kamasamudram, K., Currier, N.W., Yezerets, A.: Chemical deSO<sub>x</sub>: an effective way to recover Cu-zeolite SCR catalysts from sulfur poisoning. *Catal. Today* **267**, 10–16 (2016)
31. Wang, D., Jangjou, Y., Liu, Y., Sharma, M.K., Luo, J., Li, J., Kamasamudram, K., Epling, W.S.: A comparison of hydrothermal aging effects on NH<sub>3</sub>-SCR of NO<sub>x</sub> over Cu-SSZ-13 and Cu-SAPO-34 catalysts. *Appl. Catal. B Environ.* **165**, 438–445 (2015)
32. Auvray, X., Mihai, O., Lundberg, B., Olsson, L.: Deactivation of Cu/SSZ-13 NH<sub>3</sub>-SCR catalyst by exposure to CO, H<sub>2</sub>, and C<sub>3</sub>H<sub>6</sub>. *Catalysts* **9**, 929, (2019)
33. Supriyanto, K., Wijayanti, A., Kumar, S., Joshi, K., Kamasamudram, N.W., Currier, A., Olsson, Y.L.: A global kinetic model for hydrothermal aging of Cu zeolites used in NH<sub>3</sub> SCR. *Appl. Catal. B Environ.* **163**, 382 (2015)
34. Luo, J., Wang, D., Kumar, A., Li, J., Kamasamudram, K., Currier, N., Yezerets, A.: Identification of two types of Cu sites in Cu/SSZ-13 and their unique responses to hydrothermal aging and sulfur poisoning. *Catal. Today* **267**, 3–9 (2016)
35. Leistner, K., Mihai, O., Wijayanti, K., Kumar, A., Kamasamudram, K., Currier, N.W., Yezerets, A., Olsson, L.: Comparison of Cu/BEA, Cu/SSZ-13 and Cu/SAPO-34 for ammonia-SCR reactions. *Catal. Today* **258**, 49–55 (2015)
36. Jangjou, Y., Do, Q., Gu, Y.T., Lim, L.G., Sun, H., Wang, D., Kumar, A., Li, J.H., Grabow, L.C., Epling, W.S.: Nature of Cu active centers in Cu-SSZ-13 and their responses to SO<sub>2</sub> exposure. *ACS Catal.* **8**, 1325–1337 (2018)
37. Wei, L., Yao, D.W., Wu, F., Liu, B., Hu, X.H., Li, X.W., Wang, X.L.: Impact of hydrothermal aging on SO<sub>2</sub> poisoning over Cu-SSZ-13 diesel exhaust SCR catalysts. *Ind. Eng. Chem. Res.* **58**, 3949–3958 (2019)
38. Su, W., Chang, H., Peng, Y., Zhang, C., Li, J.: Reaction pathway investigation on the selective catalytic reduction of NO with NH<sub>3</sub> over Cu/SSZ-13 at low temperatures. *Environ. Sci. Technol.* **49**, 467–473 (2015)
39. Szanyi, J., Kwak, J.H., Zhu, H., Peden, C.H.F.: Characterization of Cu-SSZ-13 NH<sub>3</sub> SCR catalysts: an in situ FTIR study. *Phys. Chem. Chem. Phys.* **15**, 2368–2380 (2013)
40. Zhang, R., McEwen, J.-S., Kollár, M., Gao, F., Wang, Y., Szanyi, J., Peden, C.H.F.: NO chemisorption on Cu/SSZ-13: a comparative study from infrared spectroscopy and DFT calculations. *ACS Catal.* **4**, 4093–4105 (2014)
41. Ruggeri, M.P., Nova, I., Tronconi, E., Pihl, J.A., Toops, T.J., Partridge, W.P.: In-situ DRIFTS measurements for the mechanistic study of NO oxidation over a commercial Cu-CHA catalyst. *Appl. Catal. B Environ.* **166–167**, 181–192 (2015)
42. Negri, C., Hammershøi, P.S., Janssens, T.V.W., Beato, P., Berlier, G., Bordiga, S.: Investigating the low temperature formation of CuII-(N, O) species on Cu-CHA zeolites for the selective catalytic reduction of N<sub>2</sub>O. *Chem. Eur. J.* **24**, 12044–12053 (2018)
43. Bensitel, M., Saur, O., Lavalley, J.C., Mabilon, G.: Acidity of zirconium oxide and sulfated ZrO<sub>2</sub> samples. *Mater. Chem. Phys.* **17**, 249–258 (1987)
44. Burch, R., Watling, T.C.: The effect of sulphur on the reduction of NO by C<sub>3</sub>H<sub>6</sub> and C<sub>3</sub>H<sub>8</sub> over Pt/Al<sub>2</sub>O<sub>3</sub> under lean-burn conditions. *Appl. Catal. B Environ.* **17**, 131–139 (1998)
45. Waqif, M., Saad, A.M., Bensitel, M., Bachelier, J., Saur, O., Lavalley, J.C.: Comparative study of SO<sub>2</sub> adsorption on metal oxides. *J. Chem. Soc., Faraday Trans.* **88**, 2931–2936 (1992)

**Publisher's Note** Springer Nature remains neutral with regard to jurisdictional claims in published maps and institutional affiliations.